



www.sciencemag.org/cgi/content/full/science.aah6516/DC1

Supplementary Materials for

Microresonator soliton dual-comb spectroscopy

Myoung-Gyun Suh, Qi-Fan Yang, Ki Youl Yang, Xu Yi, Kerry J. Vahala*

*Corresponding author. E-mail: vahala@caltech.edu

Published 13 October 2016 on *Science* First Release
DOI: 10.1126/science.aah6516

This PDF file includes:

Materials and Methods

Supplementary Text

Fig. S1

References

Materials and Methods

Silica wedge disk resonator

The fabrication of the resonators is detailed elsewhere (29). Briefly, it proceeds as follows. An 8-micron-thick silica layer is thermally grown on a 4-inch silicon wafer and 3 mm disk patterns are defined through standard photolithographic methods. The disk patterns are transferred to a silica layer by Buffered Hydrofluoric (HF) acid etching. The diameter of the disk is controlled by the HF etching time. In cross section, the silica disks have a wedge-shaped feature at their exterior. The wedge angle is around 30 degrees. Precision control of the diameter and wedge angle enables control of modal spectra and avoided mode crossings so as to enable soliton generation (24). Finally, the silicon substrate is dry-etched using XeF_2 to create an air cladding around the wedge boundary of the disk resonator. Optical Whispering-Gallery-Modes are guided along the wedge boundary. The intrinsic quality factor is approximately 300 million. During the measurement, the resonators are overcoupled (loaded quality factor is <150 million). While these devices use a fiber taper (31,32) for optical coupling to the resonator, recently, the above silica disk fabrication process has been adapted to create a fully-integrated waveguide (33). This waveguide, based on silicon nitride, enables integration of the high-Q silica resonator with other optical components. Moreover, the structure can be integrated with microheaters to enable electrical control of spectra as has been demonstrated elsewhere (27).

Soliton generation

The solitons are generated using the active capture and locking technique (34). Here, the frequency of the pump laser is tuned towards the resonance from the lower frequencies at a speed of approximately ~ 1 GHz/ms. The pump frequency tuning is stopped before reaching the resonance and the pump power is modulated using an AOM to induce a power kick, which deterministically generates soliton steps as described elsewhere (24). A feedback loop is then turned on to selectively lock to specific soliton numbers according to their comb power levels. The linewidth of the pump lasers is ~ 2 kHz and the pump power used for a soliton generation is in the range between 200 \sim 400 mW. The generated solitons are stable indefinitely. By using the locking method described here, recordings of their properties such as average power and pulse width have been measured for over 20 hours (24). In this experiment, the two soliton combs operated stably until the system was turned off by the operators.

H^{13}CN gas cell

The H^{13}CN gas cell, which is manufactured by Wavelength References, Inc., is 16.5 cm long and pressurized to 300 Torr. The estimated linewidth of the H^{13}CN spectral features is 200 pm or approximately 25 GHz at 1550 nm.

Synthetic absorption spectra of Waveshaper

The synthetic absorption spectra were programmed into a Finisar WaveShaper 1000S. The WaveShaper required an erbium fiber amplifier to compensate its insertion loss. The WaveShaper allowed synthesis of arbitrary spectral transmission profiles to further verify the dual comb operation.

Directly measured $H^{13}CN$ spectrum by using wavelength-calibrated scanning laser

The directly measured $H^{13}CN$ absorption spectrum (upper panel in Fig. 4A) is obtained by coupling an external cavity diode laser (ECDL) into the $H^{13}CN$ gas cell and scanning the laser while monitoring the transmitted optical power. A separate signal is also tapped from the ECDL to function as a reference. The relative wavelength change of the ECDL during the scan is calibrated using a fiber Mach-Zehnder interferometer and absolute calibration is obtained using a reference laser which is locked to a molecular absorption line (Wavelength References Clarity laser). The signal passing through the gas cell and the reference transmissions are recorded simultaneously, and the absorption spectrum in Fig. 4A is extracted by dividing the signal transmission by the reference transmission.

Supplementary Text

Details on the experimental setup

A detailed diagram of the experimental setup is provided in Fig. S1. The microresonators are pumped at 1549.736 nm and 1549.916 nm using two amplified fiber lasers (Orbits Light-wave), but in principle, pumping from a single laser is possible. The difference frequency of the pumps was determined to be 22.5 GHz by detecting their electrical beat note and measurement on a spectrum analyzer. After amplification, each pump laser is coupled to an acousto-optic frequency modulator (AOM). The frequency-shifted output of the AOM is used to provide a controllable optical pumping power that is required for soliton triggering (34) as described above. The pump light is evanescently coupled into the silica microresonator via a fiber taper (31, 32). Residual pumping light that is transmitted past each resonator is filtered using a fiber Bragg grating (FBG). After the FBG, a 90/10 tap is used to monitor the soliton power for feedback control of the pump laser frequency so as to implement soliton locking (34). The optical spectra of the individual soliton streams were monitored using a Yokogawa optical spectrum analyzer. Additional precision calibration of the spectra was possible using a Wavelength References Clarity laser locked to a molecular absorption line. The two soliton pulse streams are combined in a bidirectional coupler and sent to a $H^{13}CN$ gas cell (or a WaveShaper) and a reference path. The soliton pulse streams are detected by u2t photodetectors with bandwidths of 50 GHz. The interferograms are recorded on an oscilloscope. The repetition rates of the soliton pulse streams are also monitored by an electrical spectrum analyzer (ESA).

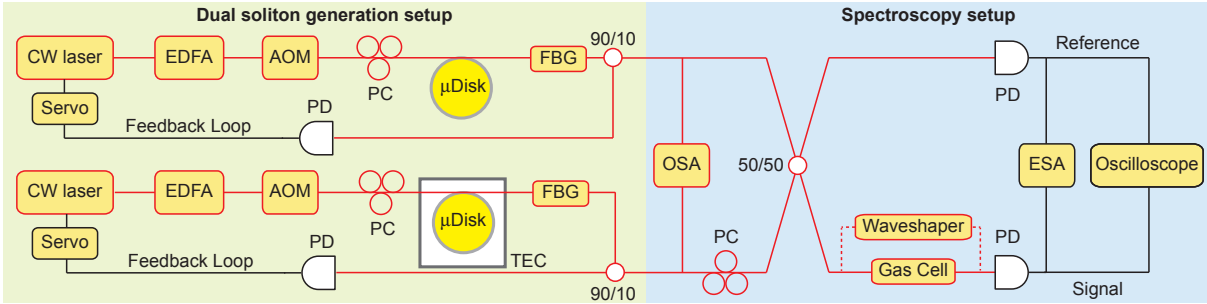


Fig. S1: Detailed experimental setup. Continuous-wave (CW) fiber lasers are amplified by erbium-doped fiber amplifiers (EDFA) and coupled into high-Q silica wedge microresonators via tapered fiber couplers. An acousto-optic modulator (AOM) is used to control pump power to trigger soliton generation in the microresonators. Polarization controllers (PC) are used to optimize resonator coupling. A fiber Bragg grating (FBG) removes the transmitted pump power in the soliton microcomb. The pump laser frequency is servo controlled to maintain a fixed detuning from the microcavity resonance by holding the soliton average power to a fixed setpoint. An optical spectrum analyzer (OSA) monitors the spectral output from the microresonators. The two soliton pulse streams are combined in a bidirectional coupler and sent to a gas cell (or a WaveShaper) and a reference path. The interferograms of the combined soliton pulse streams are generated by photodetection (PD) and recorded on an oscilloscope. The repetition rates of the soliton pulse streams are also monitored by an electrical spectrum analyzer (ESA). The temperature of one resonator is controlled by a thermoelectric cooler (TEC) to tune the optical frequency difference of the two solitons.

References

1. D. J. Jones, S. A. Diddams, J. K. Ranka, A. Stentz, R. S. Windeler, J. L. Hall, S. T. Cundiff, Carrier-envelope phase control of femtosecond mode-locked lasers and direct optical frequency synthesis. *Science* **288**, 635–640 (2000). [Medline](#)
[doi:10.1126/science.288.5466.635](https://doi.org/10.1126/science.288.5466.635)
2. R. Holzwarth, T. Udem, T. W. Hansch, J. C. Knight, W. J. Wadsworth, P. S. Russell, Optical frequency synthesizer for precision spectroscopy. *Phys. Rev. Lett.* **85**, 2264–2267 (2000). [Medline](#)
[doi:10.1103/PhysRevLett.85.2264](https://doi.org/10.1103/PhysRevLett.85.2264)
3. S. A. Diddams, T. Udem, J. C. Bergquist, E. A. Curtis, R. E. Drullinger, L. Hollberg, W. M. Itano, W. D. Lee, C. W. Oates, K. R. Vogel, D. J. Wineland, An optical clock based on a single trapped $^{199}\text{Hg}^+$ ion. *Science* **293**, 825–828 (2001). [Medline](#)
[doi:10.1126/science.1061171](https://doi.org/10.1126/science.1061171)
4. S. Schiller, Spectrometry with frequency combs. *Opt. Lett.* **27**, 766–768 (2002). [Medline](#)
[doi:10.1364/OL.27.000766](https://doi.org/10.1364/OL.27.000766)
5. F. Keilmann, C. Gohle, R. Holzwarth, Time-domain mid-infrared frequency-comb spectrometer. *Opt. Lett.* **29**, 1542–1544 (2004). [Medline](#)
[doi:10.1364/OL.29.001542](https://doi.org/10.1364/OL.29.001542)
6. I. Coddington, W. C. Swann, N. R. Newbury, Coherent multiheterodyne spectroscopy using stabilized optical frequency combs. *Phys. Rev. Lett.* **100**, 013902 (2008). [Medline](#)
[doi:10.1103/PhysRevLett.100.013902](https://doi.org/10.1103/PhysRevLett.100.013902)
7. P. Giaccari, J.-D. Deschênes, P. Saucier, J. Genest, P. Tremblay, Active Fourier-transform spectroscopy combining the direct RF beating of two fiber-based mode-locked lasers with a novel referencing method. *Opt. Express* **16**, 4347–4365 (2008). [Medline](#)
[doi:10.1364/OE.16.004347](https://doi.org/10.1364/OE.16.004347)
8. B. Bernhardt, A. Ozawa, P. Jacquet, M. Jacquy, Y. Kobayashi, T. Udem, R. Holzwarth, G. Guelachvili, T. W. Hänsch, N. Picqué, Cavity-enhanced dual-comb spectroscopy. *Nat. Photonics* **4**, 55–57 (2010). [doi:10.1038/nphoton.2009.217](https://doi.org/10.1038/nphoton.2009.217)
9. T. Ideguchi, A. Poisson, G. Guelachvili, N. Picqué, T. W. Hänsch, Adaptive real-time dual-comb spectroscopy. *Nat. Commun.* **5**, 3375 (2014). [doi:10.1038/ncomms4375](https://doi.org/10.1038/ncomms4375)
10. I. Coddington, N. Newbury, W. Swann, Dual-comb spectroscopy. *Optica* **3**, 414 (2016).
[doi:10.1364/OPTICA.3.000414](https://doi.org/10.1364/OPTICA.3.000414)
11. P. Del’Haye, A. Schliesser, O. Arcizet, T. Wilken, R. Holzwarth, T. J. Kippenberg, Optical frequency comb generation from a monolithic microresonator. *Nature* **450**, 1214–1217 (2007). [Medline](#)
[doi:10.1038/nature06401](https://doi.org/10.1038/nature06401)
12. T. J. Kippenberg, R. Holzwarth, S. A. Diddams, Microresonator-based optical frequency combs. *Science* **332**, 555–559 (2011). [Medline](#)
[doi:10.1126/science.1193968](https://doi.org/10.1126/science.1193968)

13. I. S. Grudinin, N. Yu, L. Maleki, Generation of optical frequency combs with a CaF₂ resonator. *Opt. Lett.* **34**, 878–880 (2009). [Medline doi:10.1364/OL.34.000878](#)
14. S. B. Papp, S. A. Diddams, Spectral and temporal characterization of a fused-quartz-microresonator optical frequency comb. *Phys. Rev. A* **84**, 053833 (2011). [doi:10.1103/PhysRevA.84.053833](#)
15. Y. Okawachi, K. Saha, J. S. Levy, Y. H. Wen, M. Lipson, A. L. Gaeta, Octave-spanning frequency comb generation in a silicon nitride chip. *Opt. Lett.* **36**, 3398–3400 (2011). [Medline doi:10.1364/OL.36.003398](#)
16. J. Li, H. Lee, T. Chen, K. J. Vahala, Low-pump-power, low-phase-noise, and microwave to millimeter-wave repetition rate operation in microcombs. *Phys. Rev. Lett.* **109**, 233901 (2012). [Medline doi:10.1103/PhysRevLett.109.233901](#)
17. B. Hausmann, I. Bulu, V. Venkataraman, P. Deotare, M. Lončar, Diamond nonlinear photonics. *Nat. Photonics* **8**, 369–374 (2014). [doi:10.1038/nphoton.2014.72](#)
18. T. J. Kippenberg, S. M. Spillane, K. J. Vahala, Kerr-nonlinearity optical parametric oscillation in an ultrahigh-Q toroid microcavity. *Phys. Rev. Lett.* **93**, 083904 (2004). [Medline doi:10.1103/PhysRevLett.93.083904](#)
19. A. A. Savchenkov, A. B. Matsko, D. Strekalov, M. Mohageg, V. S. Ilchenko, L. Maleki, Low threshold optical oscillations in a whispering gallery mode CaF₂ resonator. *Phys. Rev. Lett.* **93**, 243905 (2004). [Medline doi:10.1103/PhysRevLett.93.243905](#)
20. A. Hugi, G. Villares, S. Blaser, H. C. Liu, J. Faist, Mid-infrared frequency comb based on a quantum cascade laser. *Nature* **492**, 229–233 (2012). [Medline doi:10.1038/nature11620](#)
21. G. Villares, A. Hugi, S. Blaser, J. Faist, Dual-comb spectroscopy based on quantum-cascade-laser frequency combs. *Nat. Commun.* **5**, 5192 (2014). [doi:10.1038/ncomms6192](#)
22. M. Yu, Y. Okawachi, A. Griffith, M. Lipson, A. L. Gaeta, Silicon-microresonator-based mid-infrared dual-comb source. In *CLEO: Science and Innovations 2016* (Optical Society of America, 2016), paper JTh4B.5. [doi:10.1364/CLEO_AT.2016.JTh4B.5](#)
23. T. Herr, V. Brasch, J. D. Jost, C. Y. Wang, N. M. Kondratiev, M. L. Gorodetsky, T. J. Kippenberg, Temporal solitons in optical microresonators. *Nat. Photonics* **8**, 145–152 (2014). [doi:10.1038/nphoton.2013.343](#)
24. X. Yi, Q.-F. Yang, K. Y. Yang, M.-G. Suh, K. Vahala, Soliton frequency comb at microwave rates in a high-Q silica microresonator. *Optica* **2**, 1078 (2015). [doi:10.1364/OPTICA.2.001078](#)
25. V. Brasch, M. Geiselmann, T. Herr, G. Lihachev, M. H. Pfeiffer, M. L. Gorodetsky, T. J. Kippenberg, Photonic chip-based optical frequency comb using soliton Cherenkov radiation. *Science* **351**, 357–360 (2016). [Medline doi:10.1126/science.aad4811](#)

26. P.-H. Wang, J. A. Jaramillo-Villegas, Y. Xuan, X. Xue, C. Bao, D. E. Leaird, M. Qi, A. M. Weiner, Intracavity characterization of micro-comb generation in the single-soliton regime. *Opt. Express* **24**, 10890–10897 (2016). [Medline doi:10.1364/OE.24.010890](#)
27. C. Joshi, J. K. Jang, K. Luke, X. Ji, S. A. Miller, A. Klenner, Y. Okawachi, M. Lipson, A. L. Gaeta, Thermally controlled comb generation and soliton modelocking in microresonators. *Opt. Lett.* **41**, 2565–2568 (2016). [Medline doi:10.1364/OL.41.002565](#)
28. See supplementary materials on *Science Online*.
29. H. Lee, T. Chen, J. Li, K. Y. Yang, S. Jeon, O. Painter, K. J. Vahala, Chemically etched ultrahigh-Q wedge-resonator on a silicon chip. *Nat. Photonics* **6**, 369–373 (2012). [doi:10.1038/nphoton.2012.109](#)
30. K. Y. Yang, K. Beha, D. C. Cole, X. Yi, P. Del’Haye, H. Lee, J. Li, D. Y. Oh, S. A. Diddams, S. B. Papp, K. J. Vahala, Broadband dispersion-engineered microresonator on a chip. *Nat. Photonics* **10**, 316–320 (2016). [doi:10.1038/nphoton.2016.36](#)
31. M. Cai, O. Painter, K. J. Vahala, Observation of critical coupling in a fiber taper to a silica-microsphere whispering-gallery mode system. *Phys. Rev. Lett.* **85**, 74–77 (2000). [Medline doi:10.1103/PhysRevLett.85.74](#)
32. S. M. Spillane, T. J. Kippenberg, O. J. Painter, K. J. Vahala, Ideality in a fiber-taper-coupled microresonator system for application to cavity quantum electrodynamics. *Phys. Rev. Lett.* **91**, 043902 (2003). [Medline doi:10.1103/PhysRevLett.91.043902](#)
33. K. Y. Yang, D. Y. Oh, S. H. Lee, K. J. Vahala, Ultra-high-Q silica-on-silicon ridge-ring-resonator with an integrated silicon nitride waveguide. In *CLEO: QELS Fundamental Science* (Optical Society of America, 2016), paper JTh4B.7. [doi:10.1364/CLEO_AT.2016.JTh4B.7](#)
34. X. Yi, Q.-F. Yang, K. Youl Yang, K. Vahala, Active capture and stabilization of temporal solitons in microresonators. *Opt. Lett.* **41**, 2037–2040 (2016). [Medline doi:10.1364/OL.41.002037](#)